Effects of Viscosity on Transonic-Aerodynamic and Aeroelastic Characteristics of Oscillating Airfoils

P Guruswamy* and P M Goorjian†
NASA Ames Research Center, Moffett Field, California

Studies were made to investigate the effects of viscosity on aerodynamic and aeroelastic characteristics of oscillating airfoils The computer code LTRAN2 (viscous), which is based on a small disturbance aerodynamic theory, was used to make aerodynamic computations. Two viscous models, the viscous-ramp model and the lag entrainment model, were considered The unsteady viscous effects were obtained by use of the quasisteady assumptions Two cases, a conventional airfoil (NACA 64A010) and a supercritical airfoil (MBB A3), were studied at Mach numbers 0 796 and 0 7557, respectively For both of the airfoils, steady and unsteady aerodynamic computations were made using inviscid and viscous theories The steady and unsteady results for the NACA 64A010 airfoil and the steady results for the MBB A3 airfoil were compared with the available wind tunnel results Flutter speeds were computed for both airfoils using the $U\,g$ method, and the effects of viscosity on the airfoils were studied Results from the viscous methods show improvement over the inviscid method

Nomenclature

a	= distance between midchord and elastic axis measured in semichords, positive toward the trailing edge
$b\ c$	= semichord and full-chord lengths, respectively
$C_{lh}\ C_{l\alpha}$	= sectional lift coefficient due to plunging and pitching modes, respectively
$C_{mh}\ C_{m\alpha}$	= sectional moment coefficient due to plunging and pitching modes, respectively
C_p	= pressure coefficient
g	= structural damping
h	= plunging displacement of elastic axis
k	= reduced frequency defined as $\omega c/U$
m	= mass of the airfoil
M_∞	= freestream Mach number
N	= number of time steps per cycle
r_α	= radius of gyration about elastic axis
U	= freestream velocity
$\bar{U}$	= nondimensionalized flutter speed, $U/b\omega_\alpha$
x_α	= distance in semichords measured from elastic axis to mass center of the airfoil, positive rearward
α	= rotation of the airfoil about the elastic axis
γ	= ratio of specific heats
δ	= ratio of maximum thickness to chord of the airfoil
λ	= flutter eigenvalue
μ	= airfoil to air mass density ratio, $m/\pi\rho b^2$
ξ	= nondimensional plunging displacement h/b
ρ	= freestream density
ϕ	= disturbance velocity potential
$\omega_h\ \omega_\alpha$	= uncoupled natural frequencies of plunging and pitching modes respectively
ω_r	= reference frequency set to unity

Presented as Paper 83 0888 at the AIAA/ASME/ASCE/AHS 24th Structures Structural Dynamics and Materials Conference Lake Tahoe, Nev , May 2 4 1983; received Sept 10 1983; revision received April 16 1984 This paper is declared a work of the U S Government and therefore is in the public domain

*Principal Analyst, Informatics General Corp , Palo Alto California Member AIAA
†Research Scientist Member AIAA

Introduction

DURING the last decade various unsteady transonic codes have been developed based on inviscid, small disturbance theory For example, LTRAN2,[1] a code based on a time integration method, is in routine use for generating unsteady transonic airloads for oscillating airfoils which are used in applications to aeroelasticity [2] Recently, attempts have been made to incorporate viscous corrections into in viscid codes The research in this paper evaluates and demonstrates the application of LTRAN2 (viscous) to aerodynamic and aeroelastic computations

Inviscid codes can provide a reasonable physical description for cases in which viscous effects are not significant Viscous effects, when significant, can cause 1) an altering of shock strength and location because of shock/boundary layer interaction, 2) camber modifications because of differences in the boundary layer displacement on the upper and lower airfoil surfaces, and 3) displacement and camber effects near the wake These viscous effects may also influence aeroelastic characteristics. A solution for more exact flow equations than the small disturbance equation is required to account for these phenomena accurately However, solving such exact equations may limit the applications because of the com putational effort required Thus, methods that are com putationally feasible are required to account for the viscosity

In Ref 3, Rizzetta developed procedures for the com putation of unsteady transonic flows including viscous ef fects In his work, LTRAN2 (inviscid)[1] was modified to account for viscous effects without penalizing the present computational efficiency of the code Two viscous models, the viscous ramp model[4] and the Green lag entrainment model[5] were considered. The basis for the development of the viscous ramp model, which is semiempirical, is the ob servation in many experimental measurements that the postshock pressure for turbulent flow over an airfoil corresponds approximately to that of the oblique shock produced by flow over a ramp with the wedge slope equal to the "detachment angle " For many flows of interest, the use of the ramp model alone will suffice to predict unsteady pressure distributions When viscous effects are significant the ramp is used in conjunction with an integral boundary layer calculation over the rearward portion of the airfoil and wake For this purpose, "lag entrainment equations," which

have been found useful for the prediction of turbulent shear layers, are employed The lag entrainment model, which is more exact, is based on the boundary layer assumption that the normal extent of the viscous region is small when com pared with airfoil or wake thickness, which necessarily applies to flows at high Reynolds numbers Both models were in corporated in LTRAN2 under quasisteady assumptions Applications were made to steady and unsteady aerodynamic computations on the RAE 2822 and NLR 7301 airfoils, and the results are compared with the experiments

Reference 3 presents a new tool developed for aeroelasticians who are looking for unsteady aerodynamic coefficients that account for viscous effects From the study made in Ref 3 it was evident that the wedge model compared better with the experiment for the NLR 7301 airfoil, whereas the lag-entrainment model compared better with the ex periment for the RAE 2822 airfoil Also, the unsteady solution from the lag entrainment model for the NLR 7301 airfoil appears to disagree with the experiment Thus, it is not clear what model should be selected for a given case, or why the lag-entrainment method compared poorly with the ex periment, particularly in the unsteady results To be able to make a correct judgement, there is a need to study more airfoils and compare them with the experiment It is in teresting to note the effect of viscosity on aeroelastic characteristics, which was not studied in Ref 3 The discussion during the aeroelasticity section in the 23rd Structures, Structural Dynamics and Materials Conference indicated the need for this type of study The present paper is an effort to evaluate the viscous models further by comparing them with experiments and to study the effect of viscosity on aeroelastic characteristics

In this work two airfoils, a conventional airfoil, NACA 64A010, and a supercritical airfoil (designed by Messer schmitt Bolkow Blohm of the Federal Republic of Germany), MBB-A3, were studied Both these airfoils have been selected by AGARD as standard airfoils for aerodynamic and aeroelastic computations [6] Coordinates for these two airfoils are taken from Ref 6 For the NACA 64A010 airfoil, steady and unsteady experimental results are available in Ref 7 For the MBB A3 airfoil, steady experimental results are available in Ref 8

For the NACA 64A010 airfoil, steady and unsteady aerodynamic results were obtained at $M=0\ 796$ using methods based on inviscid, viscous-ramp, and viscous-lag entrainment theories Pressure and force aerodynamic coefficients are compared with wind tunnel results Based on the unsteady aerodynamic coefficients obtained from the theories and the experiment, flutter speeds were computed by using the $U\,g$ method [2] Similar studies were made for the MBB-A3 airfoil at $M=0\ 7557$ Only the steady state results were compared with the wind tunnel experiment because unsteady wind tunnel results were not available Also, flutter results from experiment were not available for both of the airfoils

Aerodynamic Equations of Motion

The inviscid, low frequency, unsteady, small perturbation potential equation considered is

$$\left(\frac{2kM_\infty^2}{\delta^{2/3}}\right)\phi_{xt}=\left[\left(\frac{1-M_\infty^2}{\delta^{2/3}}\right)-(\gamma+1)M_\infty^m\phi_x\right]\phi_{xx}+\phi_{yy} \quad (1)$$

where the exponent m is defined based on modified Krupp scaling [1]

If the airfoil surface is defined as $y^\pm=\delta^{2/3}f(x)^\pm$, the flow tangency condition is

$$\phi_y^\pm=f_x^\pm \quad \text{on} \quad y=0^\pm \qquad \text{for} \quad 0\le x\le 1 \quad (2)$$

The jump condition across the trailing vortex wake is

$$[\phi_y]=0 \quad \text{on} \quad y=0 \qquad x>1 \quad (3)$$

Equation (1) is solved by LTRAN2 by using a time accurate, alternating direction, implicit finite difference scheme [1] To account for viscous effects in conjunction with inviscid Eq (1), two procedures, a viscous ramp method and a lag entrainment method, are considered

The viscous ramp procedure[9] is a phenomenological method in which a priori determined shape changes simulating the viscous displacement effects are incorporated into the inviscid procedure Here the shock/boundary layer interaction is modeled by placing a wedge nosed ramp at the base of the shock to obtain the reduced shock pressure rise The appropriate wedge angle is determined via the shock polar using a postulated postshock pressure based upon measurements Other features of the wedge ramp as well as its placement relative to the shock profile are developed based on suitable steady, measured pressure distributions Augmenting the surface geometry by the ramp model results in the following modification to the small disturbance tangency condition defined in Eq (2):

$$\phi_y^\pm=f_x^\pm+f_{R_x}^\pm \quad \text{on} \quad y=0^\pm \quad \text{for} \quad 0\le x\le 1 \quad (4)$$

where f_x is the slope of the airfoil and f_{R_x} the correction due to viscous effects using the ramp model Details of the computation of f_{R_x} can be found in Ref 3

The ramp model which is derived for steady state com putation is incorporated into unsteady computations in a quasisteady fashion The quantities required in advance to compute f_{R_x} at time level t_{n+1} are obtained from time level t_n Thus, the ramp model is valid for low frequencies

The viscous ramp model requires minimal additional computing time since it does not involve solving any dif ferential equations A more refined procedure would require appropriate differential equations to describe the viscous flow However, any such procedure should require minimal computing time to be practically useful Here, an integral set of equations, the "lag-entrainment equations,"[10] are con sidered The integral set of equations is chosen over the differential set of equations for the following two reasons: 1) integral techniques generally require considerably less computing time than the differential methods, and 2) dif ferential methods have not as yet proven to be substantially superior for the computation of flows of practical interest. The lag entrainment equations considered here have proven to be a successful computational tool for performing com pressible and incompressible boundary layer and wake calculations involving both separated and unseparated flow regions

The lag entrainment equations are predicated upon the boundary layer assumption that the normal extent of the viscous region is small when compared with airfoil or wake thickness, which necessarily applies to flows at high Reynolds numbers By integrating the governing partial differential equations in the normal direction and suitably modeling the requisite relationships, a set of three first order ordinary differential equations, "lag entrainment equations," is obtained These equations modify the original small disturbance surface tangency conditions defined in Eq (2) as

$$\phi_y^\pm=f_x^\pm+(F_1+F_2\phi_{xx})^\pm \quad \text{on} \quad y=0^\pm \qquad \text{for} \quad 0\le x\le 1 \quad (5)$$

and the downstream wake condition defined in Eq (3) as

$$[\phi_y]=[F_1+F_2\phi_{xx}] \quad \text{on} \quad y=0 \qquad \text{for} \quad x>1 \quad (6)$$

where the values of F_1 and F_2 are obtained by solving the lag-entrainment equations Details can be found in Ref 3

The lag-entrainment equations which are derived for steady state computations are incorporated for unsteady computations in a quasisteady fashion As was done for the ramp model, the information required for the time level t_{n+1}, is obtained from time level t_n Thus, this procedure is restricted to low frequencies

Both the viscous ramp and lag entrainment methods were incorporated in LTRAN2 by Rizzetta [3] In the present analysis, computations are made by using the final production version of LTRAN2 (viscous) which was prepared at NASA Ames Research Center, and by using several other improvements such as a monotone[11] algorithm, which is more stable than the original method of Murman and Cole

Aeroelastic Equations of Motion

Both coupled and uncoupled procedures have been used to compute flutter speeds in the transonic regime [2] In the coupled procedure the aerodynamic and structural equations of motion are solved simultaneously to obtain dynamic time responses Flutter speeds are obtained from a neutrally stable response. In the uncoupled procedure, a neutrally stable condition is assumed, and then the aerodynamic and aeroelastic equations of motion are solved separately Also, the assumption of the superposition of airloads for different modal motions[7 2] is made First, the aerodynamic equations are solved for given modes of motion, then the aeroelastic equations are solved using these aerodynamic results as input This procedure yields a set of eigenvalue equations, which can be solved by using the $U\,g$ method

In this analysis, the uncoupled procedure presented in Ref 2 is employed to obtain flutter boundaries The airfoil is assumed to be oscillating in pitch and plunge modes The final aeroelastic equations of motion are

$$\left[\frac{\mu k^2}{4}[M]-[A]\right]\begin{Bmatrix}\xi_0\\ \\ \alpha_0\end{Bmatrix}=\lambda[K]\begin{Bmatrix}\xi_0\\ \\ \alpha_0\end{Bmatrix} \tag{7}$$

where ξ_0 and α_0 are the nondimensional amplitudes in plunge and pitch oscillations, respectively The mass matrix $[M]$, the aerodynamic matrix $[A]$, and the stiffness matrix $[K]$ are as follows:

$$[M]=\begin{bmatrix}1 & x_\alpha\\ \\ x_\alpha & r_\alpha^2\end{bmatrix} \tag{8a}$$

$$[A]=\frac{1}{\pi}\begin{bmatrix}C_{\ell h}/2 & C_{\ell\alpha}\\ -C_{mh} & -2C_{m\alpha}\end{bmatrix} \tag{8b}$$

$$[K]=\begin{bmatrix}(\omega_h/\omega_r)^2 & 0\\ \\ 0 & r_\alpha^2(\omega_\alpha/\omega_r)^2\end{bmatrix} \tag{8c}$$

The eigenvalue λ is complex and defined as

$$\lambda=\mu(1+ig)\omega_r b^2/U^2 \tag{9}$$

The aeroelastic parameters used above are defined in the Nomenclature and details are given in Ref 2 Equation (7) is solved by the $U\,g$ method to obtain the flutter boundaries

Computational Procedures

Steady and unsteady aerodynamic computations were made using the default mesh of LTRAN2, 113 points in the x direction and 97 points in the y direction, as follows First an inviscid steady-state solution was obtained by solving the flow equations by using the approximate factorization finite difference scheme (AF2) of LTRAN2 In Ref 3, the unsteady alternating direction implicit (ADI) algorithm was employed to obtain an inviscid steady solution Some numerical experiments made during this study showed that the AF2 scheme was faster and more accurate than the unsteady ADI algorithm in obtaining the inviscid steady state solution However, the unsteady ADI algorithm was used to obtain steady viscous solutions since viscous models were incorporated only in the unsteady algorithm of the code. Starting from the known inviscid solution, the steady state solution was obtained for the viscous-ramp model using the unsteady ADI algorithm The data required to model the ramp for any time step was taken from the previous time step For most of the cases considered in this work, about 2000 time steps were required to obtain a converged viscous-ramp solution Starting from the viscous ramp steady state solution, the lag entrainment steady state solution was initiated Again, the unsteady ADI algorithm was employed The boundary layer equations were integrated for each time step by using the solution obtained from the previous time step For most of the cases considered, about 2000 time steps were required to obtain the converged lag entrainment solution

Unsteady inviscid, wedge, and lag entrainment solutions were obtained by forcing the airfoil to undergo sinusoidal motion and then integrating the flow equations in time, starting from the corresponding steady state solutions obtained earlier Convergence testing was conducted to determine the number of cycles required to obtain converged results by comparing the harmonic components of the force coefficients between the consecutive cycles For all of the cases considered, about three cycles were required during which transients disappeared and a periodic solution was obtained Stability testing was conducted by increasing the number of time steps per cycle The tests indicated that both the inviscid and viscous ramp methods require about 1080 time steps per cycle, whereas the lag entrainment method requires about 6000 8000 time steps per cycle to obtain stable solution

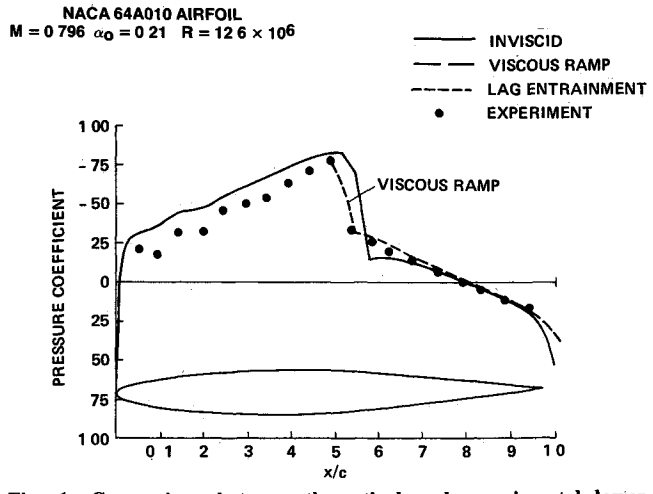

Fig 1 Comparison between theoretical and experimental lower surface steady pressure distributions

A Fourier analysis of all three solutions was performed for pressure distributions for the third cycle of oscillation, and the real and imaginary parts of the first Fourier component were extracted These results were plotted after defining the pressure as

$$C_p = \alpha_l [\text{Re} \sin \omega t - \text{Im} \cos \omega t] \quad (10)$$

where α_l is the amplitude of oscillation

Unsteady aerodynamic coefficients were computed based on the third cycle for selected values of reduced frequencies Using these coefficients, flutter speeds were computed by solving Eq (7) by the *U-g* method following the procedures described in Ref 2 Two degrees of freedom, pitching and plunging, were assumed for the aeroelastic model. Since the viscous methods considered were based on the quasisteady assumption, only low reduced frequencies (reduced frequency k based on full chord less than about 0 2) were considered for computing the flutter speeds

Results

NACA 64A010 Airfoil

In Ref 7, steady and unsteady aerodynamic results ob tained in the NASA Ames 11 $\times$ 11-ft Transonic Wind Tunnel for the NACA 64A010 airfoil are given for various flow conditions In this study, results are computed and compared with wind tunnel results at Reynolds number 12 6×10^6 for Mach 0 796 and mean angle of attack of -0 21 deg. The airfoil configuration is taken from the AGARD report [6]

Inviscid steady-pressure distributions were obtained by using the AF2 method Starting from this solution, a steady viscous ramp solution was obtained which was then used as a starting solution to obtain a steady lag entrainment solution About 2000 time steps were required for both viscous solutions Figure 1 shows the lower surface, steady-pressure distributions obtained by computations and the experiment It is observed that the viscous ramp and lag entrainment methods compared better in predicting the shock location than the inviscid method. However, in front of the shock experimental pressure points are lower than they are in all three theoretical methods Behind the shock, viscous models compare better with the experiment than does the inviscid solution

Unsteady aerodynamic results were obtained for the pitch ing motion of the airfoil at four reduced frequencies, 0 05, 0 102, 0 202, and 0 302, which were considered in the ex periment The corresponding positions of the pitching axis from the leading edge were 0 249, 0 246, 0 248, and 0 254 chords, and the amplitudes of pitching motion were 1 03, 1 02, 1 02, and 1 01 deg, respectively The unsteady inviscid, viscous ramp and lag-entrainment solutions were obtained starting from the corresponding steady state solutions ob tained earlier For all of the cases considered, three cycles were required during which the transients disappeared and a periodic solution was obtained

From the studies made it was found that the inviscid and viscous ramp methods required about 720 times steps per cycle with the exception of $k = 0$ 05, which required about 1080 time steps per cycle to give a stable solution However, the lag entrainment method required about 8000 time steps per cycle to give a fairly stable solution Figure 2 shows the plots of the magnitude of the lift coefficient and the corresponding phase angle vs the number of time steps per cycle N obtained by the lag-entrainment method at four reduced frequencies Solutions become almost stable for N closer to 8000 for both magnitude and phase However, the magnitude curves for the reduced frequencies 0 05 and 0.102 show a slight diverging trend Figure 3 shows the plots of the magnitude and the corresponding phase angle of the moment coefficient measured about the leading edge vs the number of time steps per cycle for four reduced frequencies. The four sets of curves show stable solutions for N closer to 8000

In Fig 4, the plots of the magnitude and the corresponding phase angle of the lift coefficient vs the reduced frequency are shown both for results obtained by three computational methods—inviscid, viscous ramp, and lag entrainment—and for results obtained in the wind tunnel experiments.[7] It is noted that the N considered for both the inviscid and the viscous ramp methods was 2160, whereas that for lag en trainment was 8640 Results for larger values of N than required for stability were selected because they were available from the computations for the stability test The magnitude

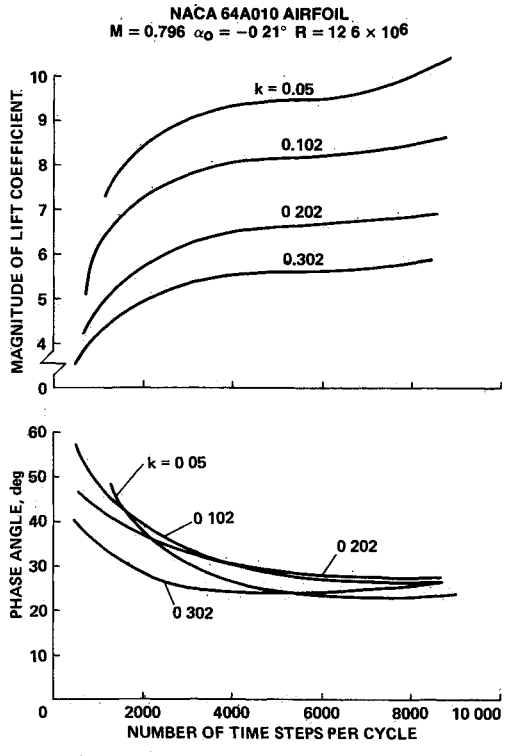

Fig. 2 Unsteady lift coefficient vs number of time steps per cycle from lag entrainment method

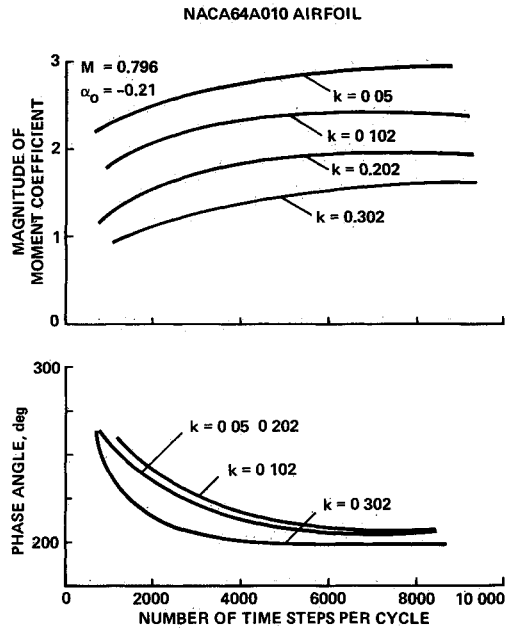

Fig 3 Unsteady moment coefficient vs number of time steps per cycle from lag entrainment method

curves show that the lag-entrainment solution is closer to the experiment when compared with the other two solutions. The viscous-ramp solution is closer to the experiment than the inviscid solution. For reduced frequencies, k less than about 0.2, the phase angle curve of the viscous-ramp solution is closer to the experiment than the other two solutions.

Figure 5 shows the magnitude and phase angle of the moment coefficient about the leading edge as a function of the reduced frequency. These results (Fig. 5) were obtained by three computational methods—inviscid, viscous-ramp, and lag-entrainment methods—in comparison with wind tunnel experiments. The magnitude curves show that the lag-entrainment solution is closer to the experiment when it is compared with the other two solutions. The viscous-ramp solution is closer to experiment than it is to the inviscid solution. The phase angle curves show that the ramp solution is closer to the experiment than the other two solutions.

A Fourier analysis of all three solutions was performed for lower surface pressure distributions for the third cycle of oscillation, and the real and imaginary parts of the first Fourier component were extracted. A comparison of these results with experiment is shown in Fig. 6. In general, the viscous solutions, particularly the lag-entrainment solution, are closer to the experiment than the inviscid solution.

Flutter speeds were computed based on the unsteady aerodynamic coefficients obtained by the computations and the experiment. They were computed by assuming the elastic axis at the quarter chord $a=-0.5$, the mass center at the midchord $x_\alpha=0.5$, and the ratio of plunge to pitch natural frequencies $\omega_h/\omega_\alpha=0.1$. In Fig. 7 the nondimensionalized flutter speed $\bar{U}$ and the corresponding reduced frequency k are shown vs the airfoil to air mass-density ratio, μ. Flutter speeds obtained by the lag-entrainment solution are closer to the experiment than the other two solutions. In general, all three theoretical methods compare fairly well with the experiment in the reduced frequency and it is observed that viscous effects have a tendency to reduce the flutter speed.

MBB-A3 Airfoil

In Ref. 8, steady-state pressure distributions measured in the blow-down wind tunnel of Aircraft Research Association Limited, Bedford, U.K., (ARA), for the MBB-A3 supercritical airfoil have been reported for various flow conditions. In this study, results were computed and compared with the experiment at a Reynolds number of 6×10^6 for a Mach number of 0.765 and a mean angle of attack of 1.5 deg, which also happens to be the design condition for the airfoil. As was done in Ref. 8, the Mach number and angle of attack considered for computations were 0.7557 and 1.30 deg, respectively, to match the flow conditions in the wind tunnel. The airfoil configuration is taken from the AGARD report.[6]

Figure 8 shows the comparison of the steady-state pressure distributions for the upper and lower surfaces. It is observed that the lag-entrainment solution compares well with the experiment. The wedge solution is closer to the experiment

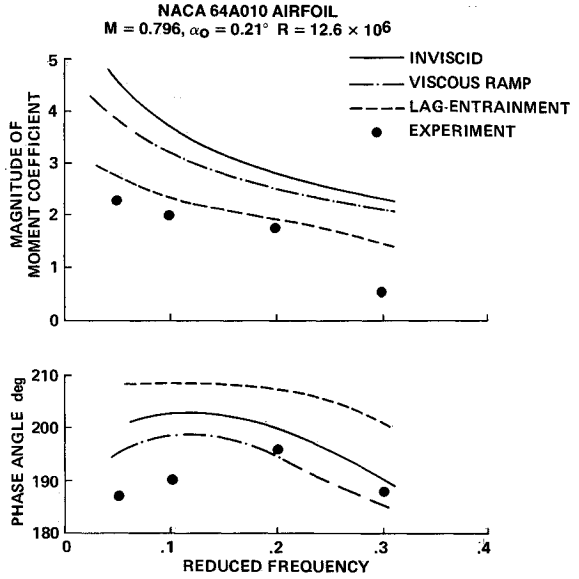

Fig. 5 Comparison between theoretical and experimental plots of moment coefficient about leading edge vs reduced frequency.

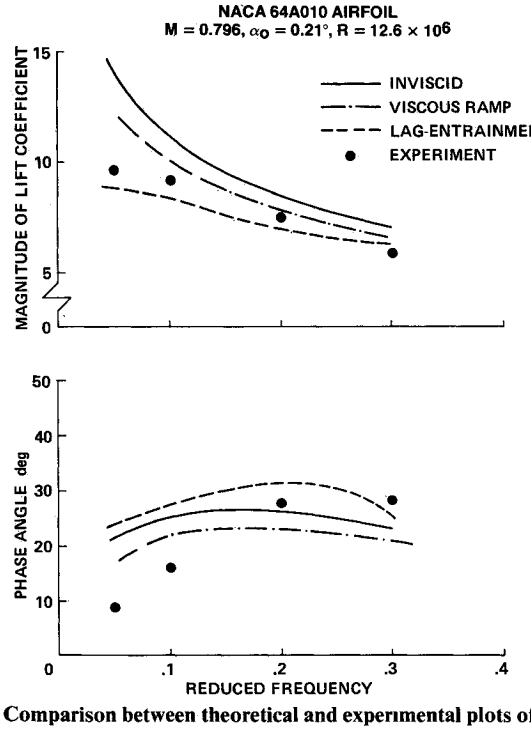

Fig. 4 Comparison between theoretical and experimental plots of lift coefficient vs reduced frequency.

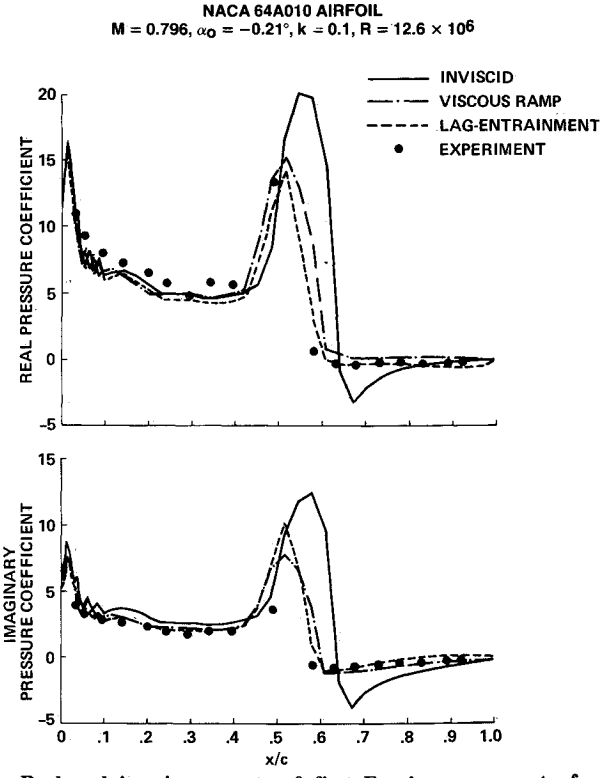

Fig. 6 Real and imaginary parts of first Fourier component of unsteady lower surface pressure coefficients.

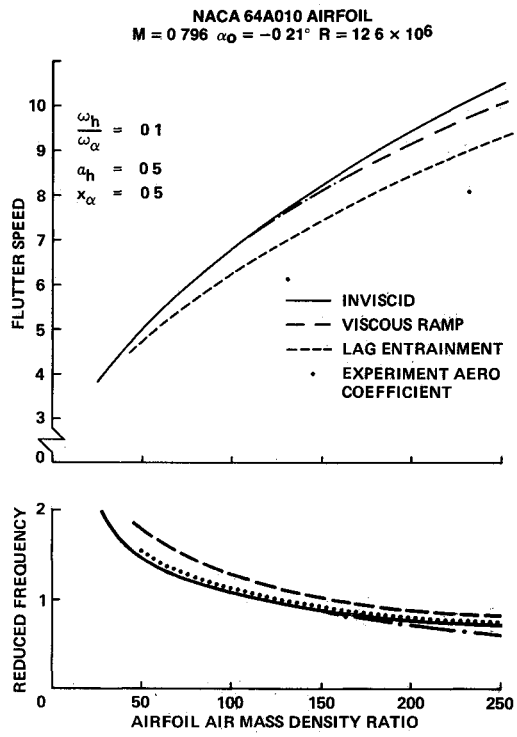

Fig 7 Comparison between theoretical and experimental flutter speeds

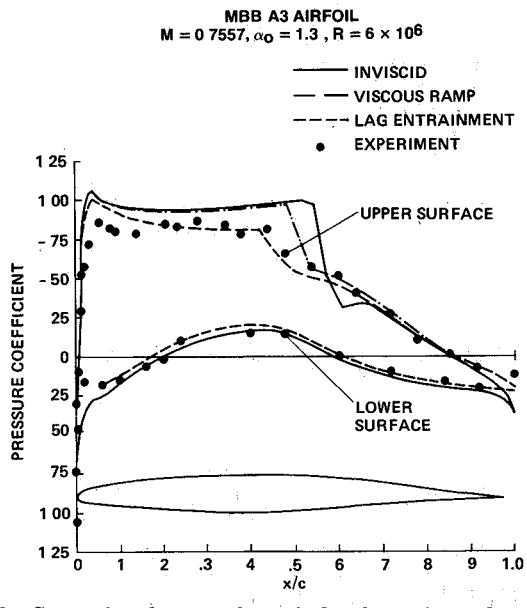

Fig 8 Comparison between theoretical and experimental upper and lower surface steady pressure distributions

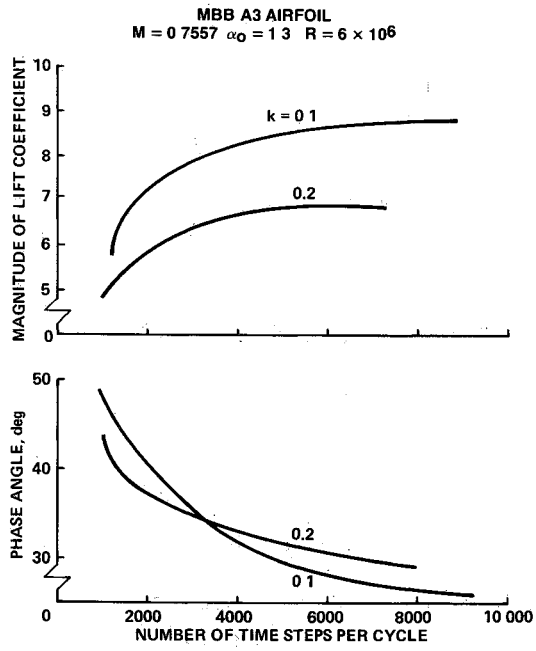

Fig 9 Unsteady lift coefficient vs number of time steps per cycle from lag entrainment method

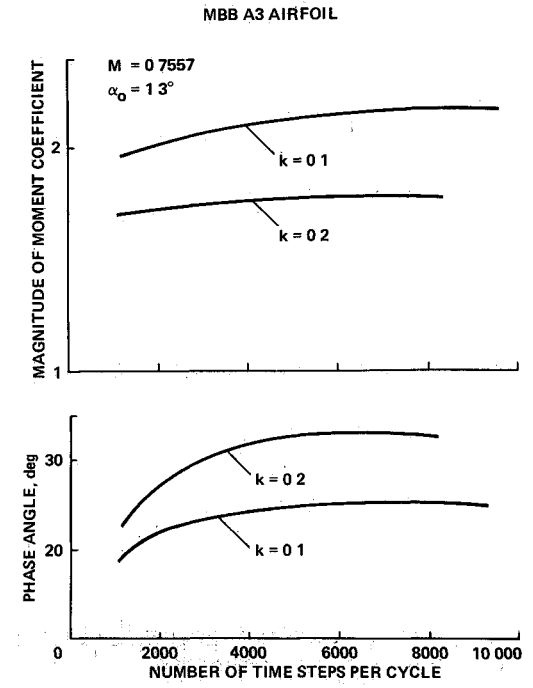

Fig 10 Unsteady moment coefficient vs number of time steps per cycle from lag-entrainment method

than the inviscid solution Steady lifts obtained by inviscid, viscous ramp lag entrainment and the experiment are 0 6667, 0 6433, 0.5377, and 0 5190, respectively

Unsteady aerodynamic results were obtained by pitching the airfoil about the midchord with an amplitude of 1.0 deg for four reduced frequencies: 0 05 0 10, 0 15, and 0 20. The unsteady inviscid, viscous-ramp, and lag entrainment solutions were obtained starting from the corresponding steady state solutions obtained earlier, For all of the cases considered three cycles were required during which the transients disappeared and a periodic solution was obtained

Studies indicated that the inviscid and viscous ramp methods required about 720 time steps per cycle with the exception of $k=0\ 05$, which required about 1080 time steps per cycle to give stable solutions However, the lag entrainment method required about 8000 time steps per cycle to give a stable solution. Figure 9 shows the plots of the magnitude of the lift coefficient and the corresponding phase angle vs the number of time steps per cycle, N, obtained by the lag entrainment method for two reduced frequencies, 0 1 and 0 2 Solutions become almost stable for N greater than 6000 for both magnitude and phase However, the code did not work for reasons not yet known during viscous computations at $k=0\ 2$ and $N=8640$ Figure 10 shows plots of the magnitude and the corresponding phase angle of the moment coefficient measured about the leading edge vs the number of

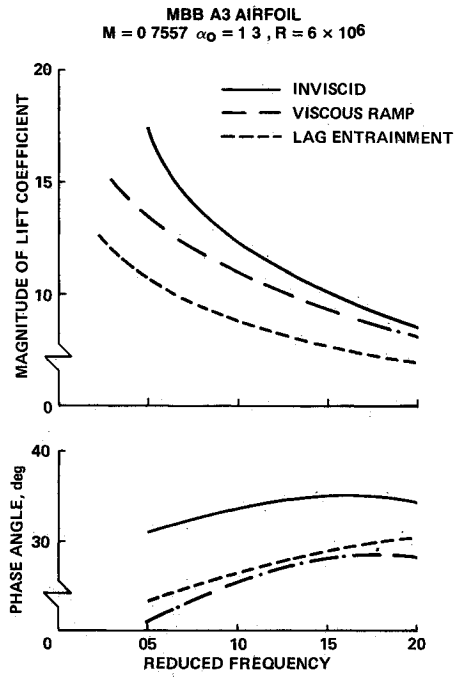

Fig 11 Comparison among theories of lift coefficient vs reduced frequency plots

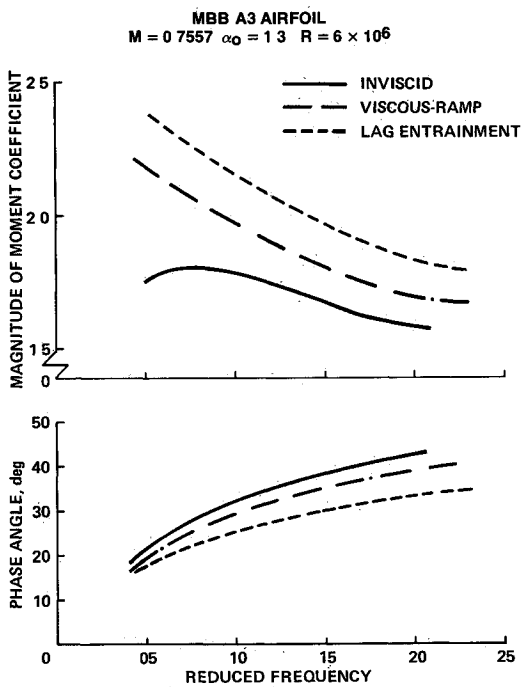

Fig 12 Comparison among theories of moment coefficient about midchord vs reduced frequency plots

time steps per cycle for two reduced frequencies These curves show the same behavior as the lift coefficient curves in Fig 9

In Fig 11, plots of the magnitude and the corresponding phase angle of the lift coefficient vs the reduced frequency are shown for results obtained by three computational methods It is noted that the number of time steps per cycle considered for both inviscid and viscous ramp methods was 2160, whereas that for the lag entrainment method was 6480 The magnitude of lift coefficients decreases in the order of the inviscid, viscous ramp, and lag entrainment solutions The phase angle curves show that viscous solutions which are fairly close give lower values than the inviscid solution

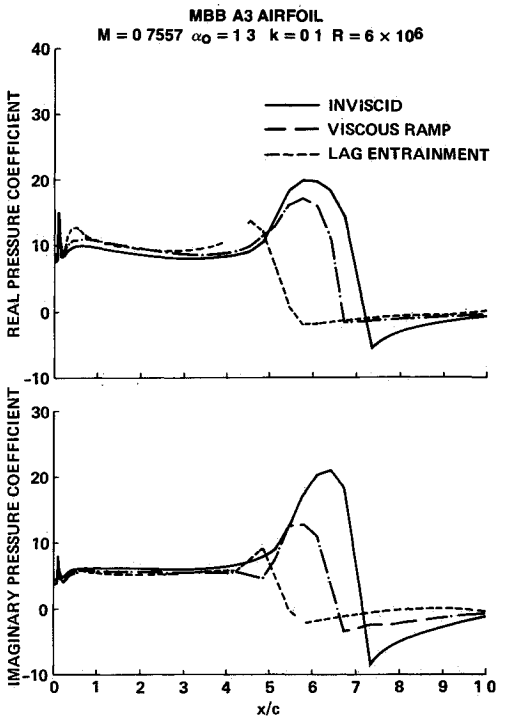

Fig 13 Real and imaginary parts of first Fourier component of unsteady upper surface pressure coefficients

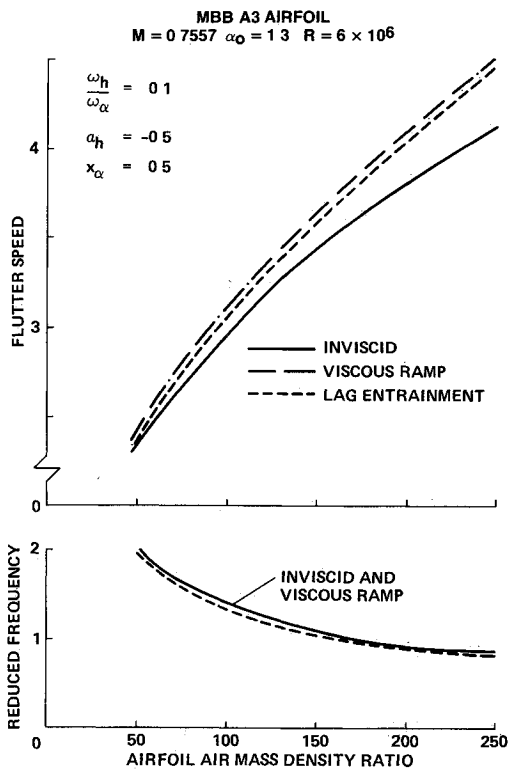

Fig 14 Comparison between theoretical and experimental flutter speeds

In Fig 12, the plots of the magnitude and the correspond ing phase angle of the moment coefficeint measured about the midchord vs the reduced frequency are shown The magnitude curves show that the values increase in the order of inviscid, viscous ramp, and lag entrainment methods The phase-angle curves show a reverse behavior

A Fourier analysis of all three solutions was performed for the upper surface pressure distributions for the third cycle of

oscillation and the real and imaginary parts of the first Fourier component were extracted A comparison of these results is shown in Fig 13 for $k=0$ 1

Flutter speeds were computed based on the unsteady aerodynamic coefficients obtaind by the three methods They were computed by assuming the elastic axis at the quarter chord $a=-0$ 5, the mass center at the midchord $x_\alpha=0$ 5, and the ratio of plunge to pitch natural frequencies $\omega_h/\omega_\alpha=0$ 1 In Fig 14, the nondimensionalized flutter speed $\bar{U}$ and the corresponding reduced frequency k are plotted vs the airfoil to air mass density ratio μ It is observed that viscous effects have a tendency to increase the flutter speed In general, the reduced frequency curves for all three theoretical methods are close

Conclusions

This paper is aimed at evaluating and demonstrating the application of a new unsteady aerodynamic tool, LTRAN2 (viscous), that will supplement inviscid computations required for application in areas such as aeroelasticity Based on the studies made, the following conclusions may be drawn:

1) Steady aerodynamic results show that viscous methods compare better with experiments than inviscid results

2) In general, unsteady results for the NACA 64A010 airfoil show that viscous methods compare better with ex periments than the inviscid theory

3) For the NACA 64A010 airfoil, flutter boundaries based on aerodynamic coefficients from the lag-entrainment method compare better with those based on experimental aerodynamic coefficients than the flutter boundaries based on the viscous ramp and inviscid methods

4) For the NACA 64A010 conventional airfoil, viscous effects decrease the values of the magnitude of lift coef ficients, the magnitude of moment coefficients about leading edge, and flutter speeds

5) For the MBB A3 supercritical airfoil, viscous effects decrease the values of the magnitude of lift coefficients, increase the magnitude of moment coefficients about mid chord, and increase flutter speeds

6) When compared with the inviscid unsteady method, the viscous ramp and the lag entrainment methods took about 0.8 and 12 1% more computational time on the CDC 7600 computer It is noted that the lag entrainment method required about four times the number of time steps per cycle than the other two methods to give a stable solution

7) Further research is required to improve viscous methods, particularly the lag entrainment method, which appear to be unstable Also, computationally efficient methods are required which will account for unsteady viscous effects without quasisteady assumptions

References

[1] Ballhaus W F and Goorjian P M Implicit Finite Difference Computations of Unsteady Transonic Flows about Airfoils *AIAA Journal* Vol 15 Dec 1977 pp 1728 1735

[2] Guruswamy P and Yang T Y Aeroelastic Time Response Analysis of Thin Airfoils by Transonic Code LTRAN2 Computers and Fluids Vol 9, No 4, Dec 1981 pp 409 425

[3] Rizzetta, D P. ' Procedures for the Computation of Unsteady Transonic Flows Including Viscous Effects NASA CR 166249 Jan 1982

[4] Rizzetta, D P and Yoshihara, H Oscillating Supercritical Airfoils in the Transonic Regime with Viscous Interaction ' *AGARD Conference Proceedings Boundary Layer Effects on Unsteady Airloads* Aix en Province, France Sept 1980

[5] Green J E Weeks D J and Merryman P J Prediction of Turbulent Boundary Layers and Wakes in Compressible Flow by a Lag Entrainment Method RAE R&M 3791 March 1977

[6] Bland S R , AGARD Two Dimensional Aeroelastic Con figurations AGARD AR 156 1979

[7] Davis S D and Malcolm G N Experimental Unsteady Aerodynamic of Conventional and Supercritical Airfoils NASA TM-81221 Aug 1980

[8] Bucciantini G Oggiano M S and Onorato, M Supercritical Airfoil MBB A3 Surface Pressure Distributions Wake and Boundary Condition Measurements ' Experimental Data Base for Computer Program Assessment AGARD AR 138 May 1979

[9] Yoshihara, H Formulation of the Three Dimensional Tran sonic Unsteady Aerodynamic Problem AFFDL TR 79 3030 Feb 1979

[10] Green J E 'Application of Head s Entrainment Method to the Prediction of Turbulent Boundary Layers and Wakes in Compressible Flow, RAE R&M 3788 April 1972

[11] Goorjian P M Meagher, M E and Van Buskirk, R , Monotone Implicit Algorithms for the Small Disturbances and Full Potential Equations Applied to Transonic Flows AIAA Paper 83 0371 Reno Nev Jan 1983